

Investigation on Metallurgical Structure and Mechanical Properties of Dissimilar Al 2024/Cu FSW T-joints

Mostaan Lotfalian Saremi¹ · Seyyed Ehsan Mirsalehi¹ · Ali Shamsipur¹

Received: 4 April 2016 / Accepted: 26 October 2016 / Published online: 10 November 2016
© The Indian Institute of Metals - IIM 2016

Abstract In this research, T-joining of AA2024-T4 and commercially pure copper were performed successfully using friction stir welding. Effect of welding parameters on metallurgical and mechanical characteristics of the joints was studied. For this purpose, tensile strength, microhardness, and macro- and microstructures of the joints were investigated. Also, the fracture surfaces were examined using XRD and SEM. The best results were obtained for the 1130 rpm rotation speed (ω) and 12 mm/min travel speed (v), with the UTS of 156 MPa ($\sim 70\%$ of Cu strength). The microhardness test showed that TMAZ and base metal of Al side had the maximum hardness amounts (148 and 155 HV, respectively). Generally, increase in the ω^2/v ratio caused the nugget zone and HAZ grain size to increase. The results revealed the formation of Al_2Cu and Al_4Cu_9 intermetallic compounds in the border zone of the joints. The fractography results showed the occurrence of cleavage fracture in all the samples.

Keywords Friction stir welding · Dissimilar T-joint · 2024 aluminum alloy · Copper · Mechanical properties · Metallurgical structure

1 Introduction

Welded T-joints are used in different industries such as supporting frames, bridge structures, buildings, etc. [1], and are generally performed by fusion welding methods

such as MIG or laser welding [2, 3]. Available fusion welding methods face a lot of difficulties for T-joining aluminum alloys such as high residual stresses, significant distortions, and metallurgical defects [4, 5]. Most of the T-joints are performed by using different situations like optimizing welding sequence and preheating to reduce welding stress and distortion [3, 6]. While the complexity of the process presents significant limitations for T-joints of aluminum alloys [7], the friction stir welding method (FSW) is an easier way to accomplish a better and faster weld [8].

Friction stir welding is a solid-state joining technology [9, 10], which was introduced in 1991 by TWI [11, 12]. At the beginning, it was used to weld non-weldable aluminum alloys [1]. This new technology was considered to have a remarkable impact due to the advantages of its energy efficiency, environmental friendliness, and versatility [13, 14]. A large range of alloys which were considered as non-weldable alloys, were successfully joined via this method (i.e. 2XXX and 7XXX series alloys) [15–17]. Nowadays, this method is used in various industries due to its economic benefits and excellent quality [1, 15].

Analysis of the T-joint of two popular aluminum alloys of 2024-T4 and 6061-T6 by FSW, and its effect on the material characteristics on joining shows that T-joints, which otherwise is characterized with poor mechanical properties via conventional welding methods, showed acceptable results [18]. Cui et al. [18] illustrated that the rising of welding speed would cause more welding defects on T-joints fabricated using three different combination modes of the skins and stringers.

One of the great advantages of the FSW method is its ability to weld dissimilar alloys to each other; the best example is the joining of aluminum alloys to copper which is applicable in electrical and aerospace industries [19, 20].

✉ Seyyed Ehsan Mirsalehi
mirsalehi@aut.ac.ir

¹ Department of Mining and Metallurgical Engineering,
Amirkabir University of Technology, P. O. Box: 15875-4413,
Tehran, Iran

Thus, considering limited previous researches regarding the FSW of T-joints, investigation on the characteristics of Al/Cu T-joints will be of significant importance.

In this paper, the FSW T-joining of 2024 aluminum alloy to pure copper has been studied, and the relationships between welding parameters, and metallurgical structure, tensile properties, micro hardness and fracture surface have been investigated.

2 Experimental

In this investigation, the T-joining of copper to aluminum was studied. A photograph of the connection is illustrated in Fig. 1. Two corner curvatures helped to reduce stress concentration on the corners of the weldment [4].

2.1 Materials and Welding Experiments

In this investigation, AA2024-T4 aluminum alloy and commercially pure copper, with thicknesses of 3 and 1 mm, respectively, were used. To perform the T-joint welding, a Swiss milling machine and also, a holding fixture (Fig. 2) were used. All of the samples were prepared with the size of 160 mm by 60 mm, and with machined edges. To ensure that no contaminants were present on the samples surfaces, the samples were cleaned with acetone. The chemical composition of the base metals was analyzed, and the results are summarized in Tables 1 and 2.

In the present investigation, the shoulder design used by Abdollah-Zadeh et al. [21] to produce sound welds on Cu/Al lap joints was employed. However, considering the low thickness of the outer skin which prevented more plunging,

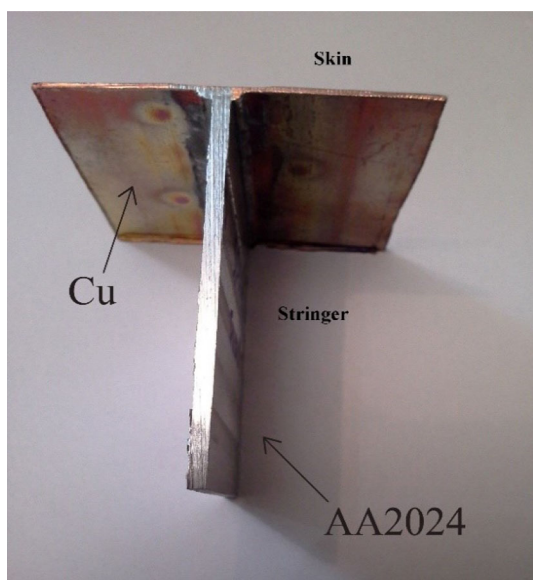


Fig. 1 Photograph of a welded T-joint

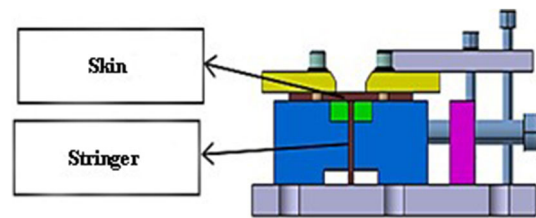


Fig. 2 Schematic of the T-Joint positioning fixture

a shoulder with a diameter of one millimeter larger was used.

In this study, the pin was produced from HSS steel, and the shoulder was prepared from SPK steel. Both of them were heat treated after the machining. Figures 3a, b show the schematics for the non-retractable simple tapered pin of 5 mm diameter and 1.69 mm length, and the shoulder of 16 mm diameter, which were used in this study.

Tan et al. [22] expressed that the rotation speed of 1100 rpm and traverse speed of 20 mm/min were the optimum parameters for their dissimilar Al/Cu FSW joining. In the present study, the welding conditions were selected based on some preliminary experiments and with consideration of Ref. [22] results. The amounts of the applied rotation and traverse speeds are listed in Table 3. The tests were performed under the tilt angle of 3 degrees for all the samples. All other variables remained constant.

After welding of the samples, the initial and final portions were discarded, and the tensile and metallographic specimens were extracted.

2.2 Metallographic Evaluation

All the samples were polished and etched according to ASTM-E3-01 [23]. It might be the first time that dissimilar materials presented in a weldment were etched together by changing the etchant and etching condition. First, Cu was etched with NH_4OH which was activated by H_2O_2 . Then, Weck's reagent solution (100 ml H_2O , 4gr KMnO_4 , and 1gr NaOH) was used for the Al alloy.

In order to study the metallurgical structure of the cross-section of the joints, a polarized Nikon optical microscope, and a Vega Scan scanning electron microscope, operating at 25 kV, equipped with energy-dispersive spectroscopy (EDS) were used.

2.3 Mechanical Testing

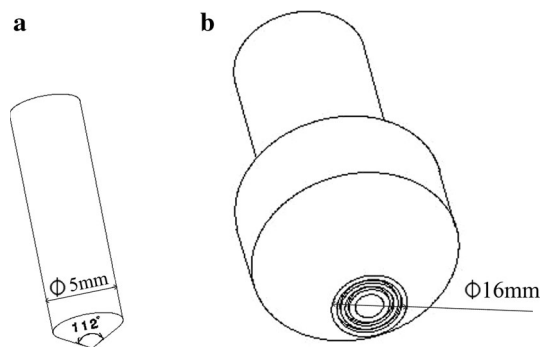
A Zwick /SO1200 universal test machine was used for tensile testing, and all the samples were examined at a 5 mm/min strain rate, according to ASTM E8/E8M [24]. The fixture, as shown in Fig. 4, was used for tensile testing.

Table 1 The result of chemical analysis of the aluminum alloy base metal (wt%)

AA2024									
Al	Cr	Ti	Zn	Si	Fe	Mn	Mg	Cu	Bal.
93.02	0.0064	0.029	0.069	0.24	0.32	0.47	1.30	4.51	0.0351

Table 2 The result of chemical analysis of the copper base metal (wt%)

Pure Cu									
Cu	Ag	As	Sb	Bi	S	P	Al	Zn	Sn
99.917	0.002	0.006	0.012	0.004	0.003	0.001	0.006	0.025	0.129

**Fig. 3** Schematics of: **a** the simple tapered pin, and **b** the shoulder**Table 3** Welding parameters used in the experiments

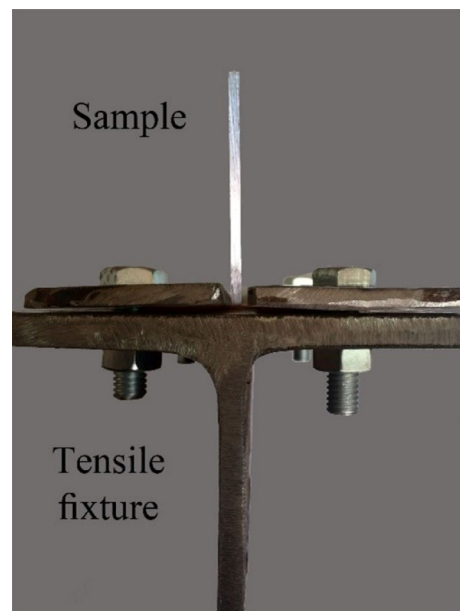
Experiment no.	Sample ID.	Rotation speed (rpm)	Rotation speed level	Travel speed (mm/min)	Travel speed level
1	R1T1	940	1	12	1
2	R1T2	940	1	18	2
3	R2T1	1130	2	12	1
4	R2T2	1130	2	18	2
5	R3T1	1340	3	12	1
6	R3T2	1340	3	18	2

2.4 Micro Hardness Testing

Micro hardness measurements were done on a linear route perpendicular to the copper, from the copper side to aluminum side. The test was performed according to ASTM E384 [25] and with a 50grf load and a 5 s dwell time.

3 Results and Discussion

Among all of the weldments, the sample R2T1 is without any tunnel defects. As shown in Fig. 5, the maximum tensile strength belongs to the sample R2T1 (~156 MPa),

**Fig. 4** Fixture used for tensile testing with a fastened sample

and the minimum reported strength belongs to the defective sample R3T2 (~60 MPa). According to the results of this study and other investigations [8, 19, 20], applying higher heat to the weld area by increasing the rotation speed or decreasing the travel speed will result in formation of more brittle intermetallic compounds, due to the supply of the energy required for their formation in the weld area. On the other hand, increasing the travel speed or decreasing the rotation speed over their normal range, can cause tunnel defects to occur, which decreases the material cross-section and introduces stress concentration sites, due to low heat input and weak material stirring. Hence, both the tunnel defects and intermetallic compounds have negative effects on the tensile strength of the joints.

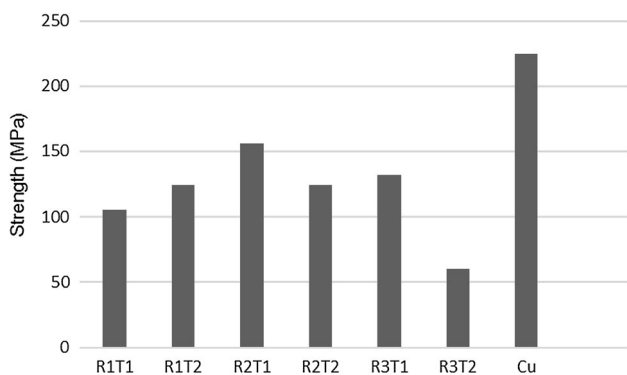


Fig. 5 Comparison of the tensile test results

Formation of intermetallic compounds is an effective phenomenon in dissimilar welding [19, 20, 26, 27]. As stated by Abbasi et al. [28], interaction of Al and Cu will cause formation of brittle intermetallics at temperatures above 120 °C. In FSW of Al/Cu dissimilar joints, the temperature experienced in the nugget zone of the weldments will be higher than this temperature. According to the measurements done using a gun thermocouple in this study, the maximum temperature experienced by the joints reaches about 440 °C. Hence, intermetallic compounds will form in this zone. However, considering the pin and joint configurations (simple tapered pin and T-joint configuration in which Cu is on the top side), two base metals can not be mixed in the weld areas, and intermetallic compounds can only be formed in the border of the two base metals. The results of EDS analysis and X-ray diffraction (XRD) of fractured surfaces confirm the presence of intermetallic compounds in the stir zones of the joints. EDS analysis results of the zones identified in the micrograph obtained from the sample R2T1 (Fig. 6) is shown in Fig. 7a, b, and the final results have been summarized in Table 4. According to the Al-Cu phase diagram (Fig. 8) and considering the welding temperature, the EDS results reveal the probable formation of Al_2Cu (θ) and Al_4Cu_9 (γ_1) intermetallic compounds. Based on the phase diagram, it is obvious that the dissolution temperatures of these compounds are higher than the welding temperature. The XRD results (Fig. 9) confirm the formation of these intermetallic compounds. The lower intensities of Al_2Cu and Al_4Cu_9 in Fig. 9a compared to Fig. 9b, reveal that there are fewer intermetallic compounds in the sample R2T1 (the strongest joint) compared to the sample R3T2 (the weakest joint). Thus, this subject can be effective in understanding resultant joint strengths.

Macroscopic image of the sample R2T1 is shown in Fig. 10. As can be seen in the figure, the four joint zones: nugget zone, TMAZ, HAZ and base metal are recognizable. Figure 11 shows the macrograph of the sample R1T2 joint containing a tunnel defect which has a negative effect

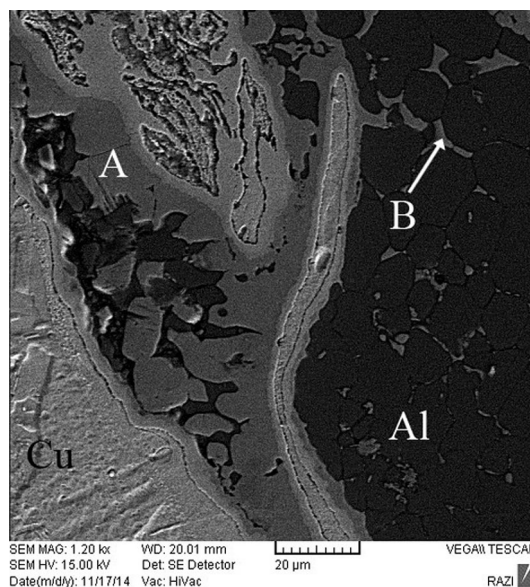


Fig. 6 SEM image of the sample R2T1 stir zone. The results of EDS analysis for the “A” and “B” zones are given in Table 4

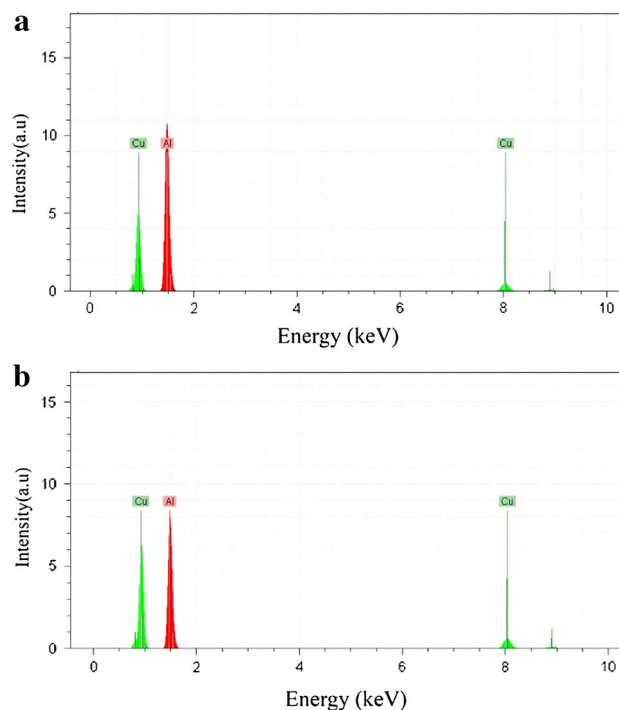


Fig. 7 EDS results of: **a** Zone A in Fig. 6, and **b** Zone B in Fig. 6

Table 4 EDS chemical analysis of the zones identified in Fig. 6

Elements	Al (at.%)	Cu (at.%)
Zone A	67.12	32.88
Zone B	29.67	70.33

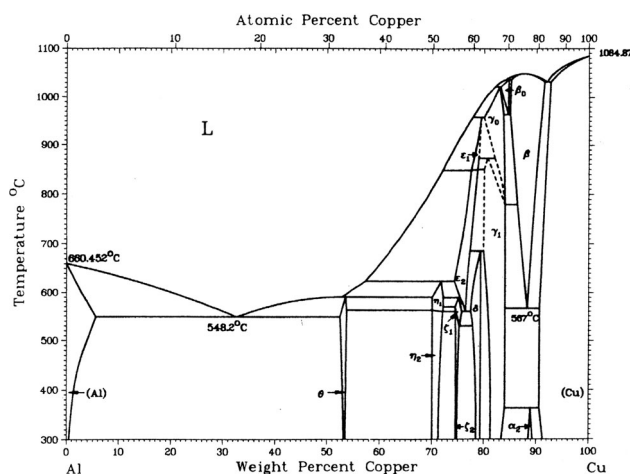


Fig. 8 Al-Cu binary phase diagram [29]

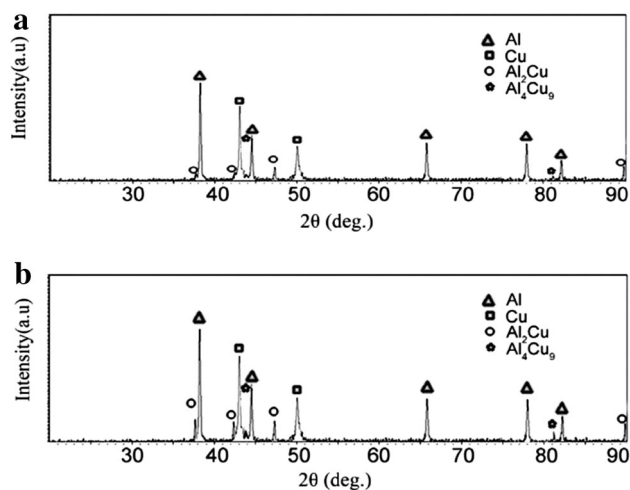


Fig. 9 XRD results confirming the formation of intermetallic compounds in: a sample R2T1, and b sample R3T2

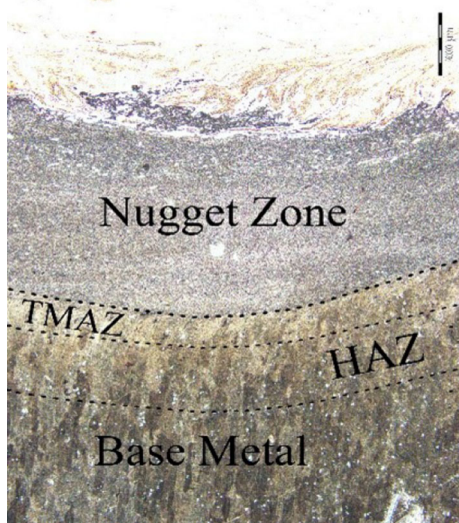


Fig. 10 Macrograph of the sample R2T1

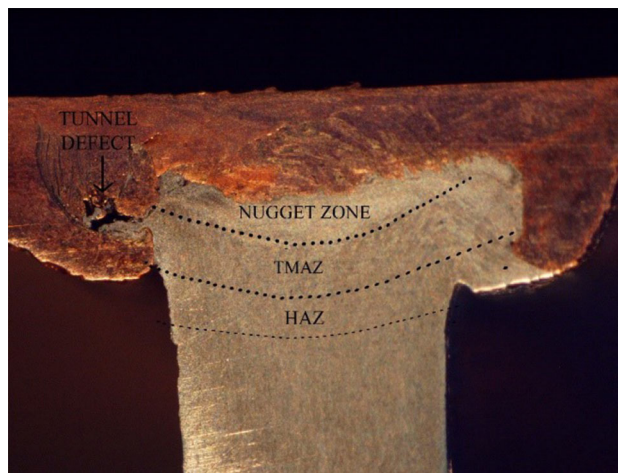


Fig. 11 Macrograph of the sample R1T2 containing a tunneling defect

on the strength. As stated by Zhao et al. [3], tunnel defects are common in FSW T-joints. In addition, considering the difficult mixing in dissimilar Al/Cu FSW joining, Tan et al. [22] and Barekatin et al. [30] have also examined the specimens containing tunnel defects in order to evaluate effect of the defects on the tensile properties of the weldments.

Figure 12 shows microstructure of the joint area of the sample R2T1. According to the image, in the interface of stirred Al and Cu, there are continuous layers with different colors stating from the base metal. Comparison of the OM images and the SEM images (Fig. 13), considering the results of EDS and XRD of fracture surface, shows that these continuous layers are intermetallic compounds that seem to be responsible for the failure of the sample. The other proof for this fact is brittle fracture observed for this sample (Fig. 14). According to Ref. [27], intermetallic compounds are brittle and cause brittle fracture. Figures 14 and 15 show cleavage fracture occurred in the samples R3T1 and R2T1, which confirm the presence of intermetallic compounds.

AA 2024 alloy is a heat treatable alloy, hence, aging or over aging can change its strength. Also, increasing the heat can cause grain growth in HAZ [31]. Moreover, this fact cannot be a failure factor since all the samples broke from the border of the two alloys which confirms our above-mentioned theory. The result of micro hardness test of the sample R2T1 is illustrated in Fig. 16. As can be seen, the hardness rises rapidly in the border zone, and TMAZ and base metal of Al alloy have maximum hardness (148 and 155 HV, respectively). It seems that lower hardness of nugget zone relative to the Al base metal is due to its precipitation dissolution, and lower hardness of the HAZ is due to its grain growth [32]. It seems that the

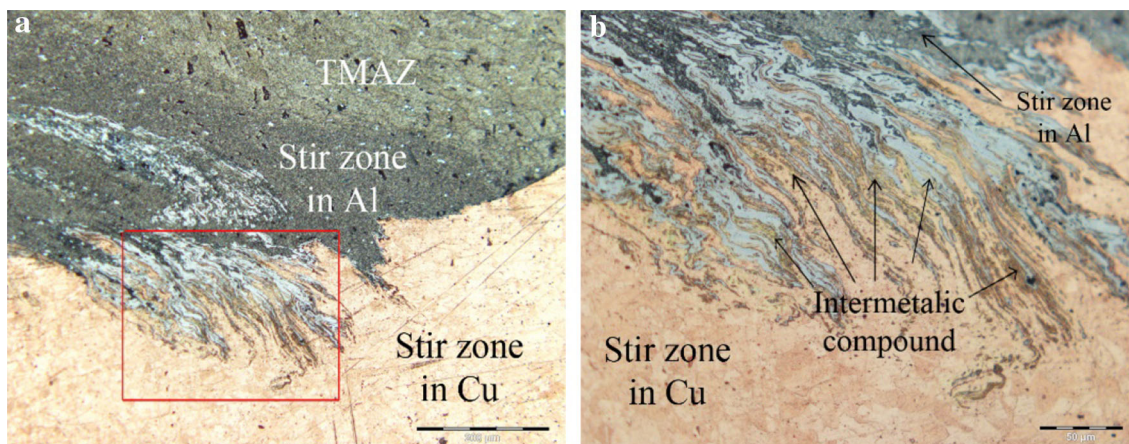


Fig. 12 Micrographs of the sample R2T1: **a** nugget zone, and **b** magnified image of the identified zone in image **a** showing the formed intermetallic compounds

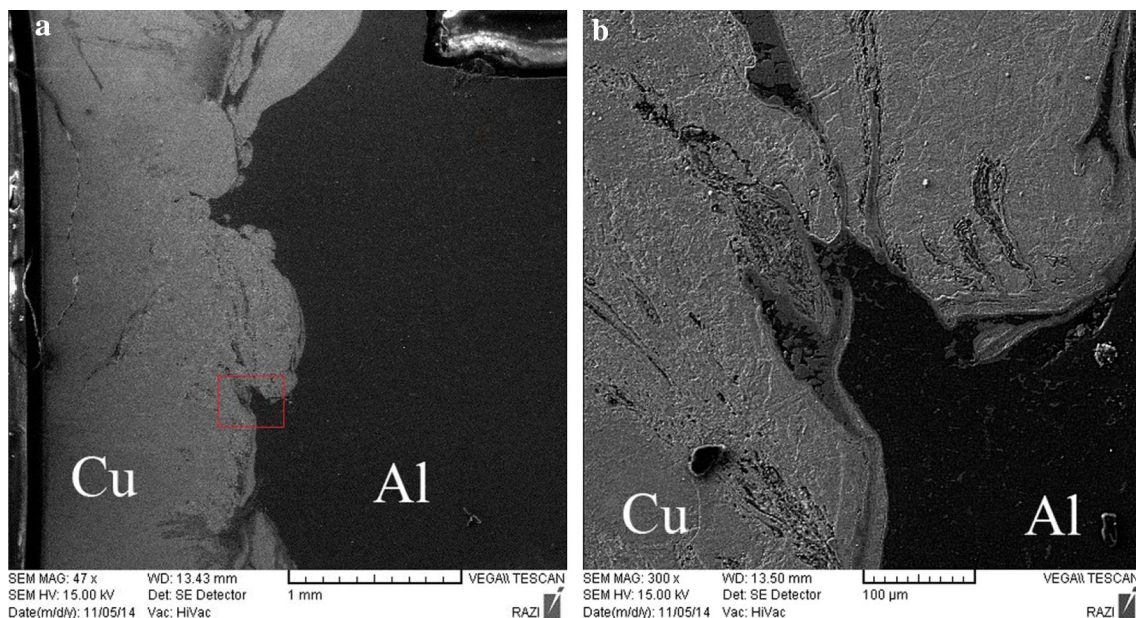


Fig. 13 **a** SEM image of the sample R2T1, and **b** magnified image of the identified zone in image (a)

increase in hardness from the HAZ to TMAZ is due to its grain stretching and work hardening in TMAZ, with consideration of experiencing both the plastic deformation and thermal cycle during FSW [33].

According to the Refs. [33, 34], the heat generated in FSW process is dependent on the rotation and travel speeds. They proposed the following function for this relationship:

$$Q \propto \frac{\omega^2}{v} \quad (1)$$

where ω displays rotation speed and v represents travel speed. The suggested function shows that higher the

rotational speed, the more is the heat generation; while on the other hand, with increasing the travel speed, the generated heat decreases. Figure 17 shows ω^2/v ratios of the experiments. As can be observed in this figure, the maximum heat is generated in R3T1.

Grain sizes of the nugget zone, TMAZ and HAZ for the sample R2T1 are shown in Table 5. According to the results, by increasing the ω^2/v ratio, the nugget zone and HAZ grain size generally increases. These grain growths are as a result of higher heat generation.

Finally, it can be concluded that the sample R2T1 has the optimum rotation and travel speeds that seems to be due to its appropriate generated heat, which makes a defect free

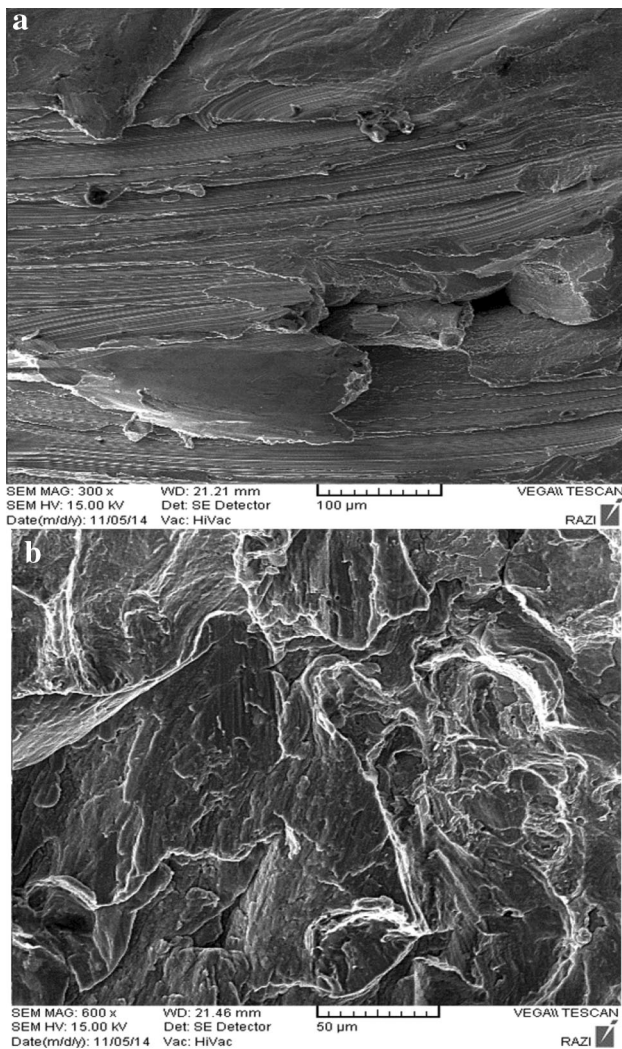


Fig. 14 Fractograph of fracture surface of the sample R3T1 with different magnifications: **a** lower magnification, and **b** higher magnification

weld and does not cause extra intermetallic formation in the border zone.

4 Conclusions

Based on the obtained results, it was revealed that FSW of Al 2024/Cu T-joints could be performed successfully. In the present paper, formation of defects and intermetallic compounds, tensile strength, micro hardness, and micro/macro structure of the joints were studied. According to the results, the following conclusions could be drawn:

1. For T-Joining of 3 mm thick AA2024 to 1 mm thick Cu with simple tapered tool pin, the best results were

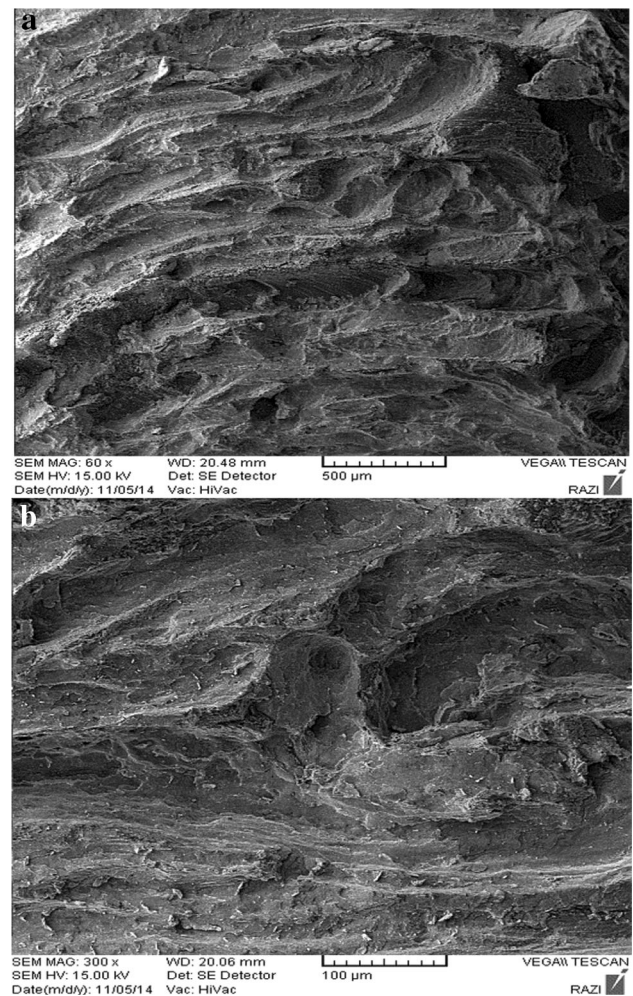


Fig. 15 Fractograph of fracture surface of the sample R2T1 with different magnifications: **a** lower magnification, and **b** higher magnification

obtained for the rotation speed of 1130 rpm and travel speed of 12 mm/min, which resulted in a defect-free weld with no extra intermetallic formation in the border zone. For this sample, the strength approached nearly 70% of the strength of the base metal, Cu (~156 MPa).

2. It seemed that occurrence of tunnel defects and formation of intermetallic compounds were responsible for decrease in the joint strength, due to welding with extra low and high heat generation, respectively.
3. According to the EDS and XRD results, the intermetallic compounds, Al_2Cu and Al_4Cu_9 were formed in the border zone of the joints.
4. Generally, increasing the ω^2/v ratio caused the nugget zone and HAZ grain size to increase.
5. The microhardness profile showed the increase in hardness from the copper side to the AA2024 side, and

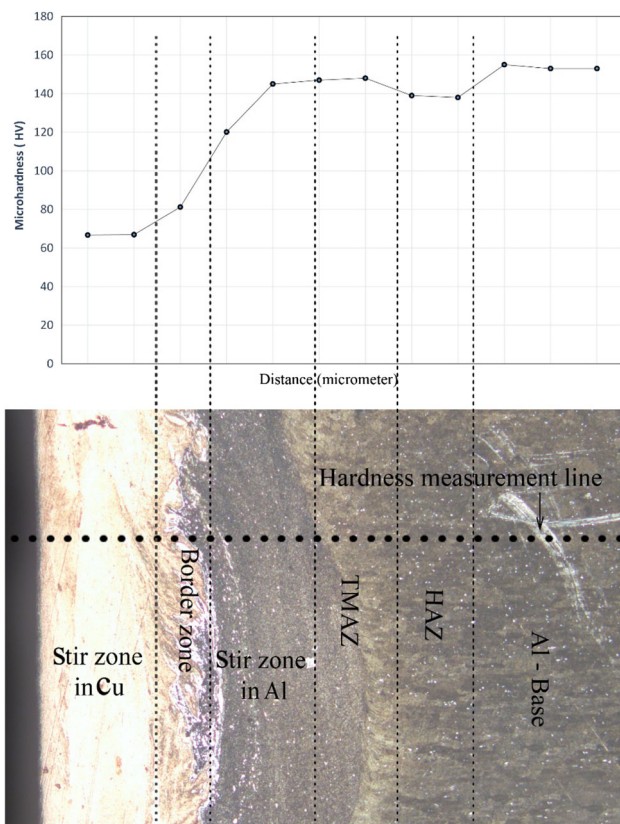


Fig. 16 Micro hardness of the sample R2T1 and the related macrograph

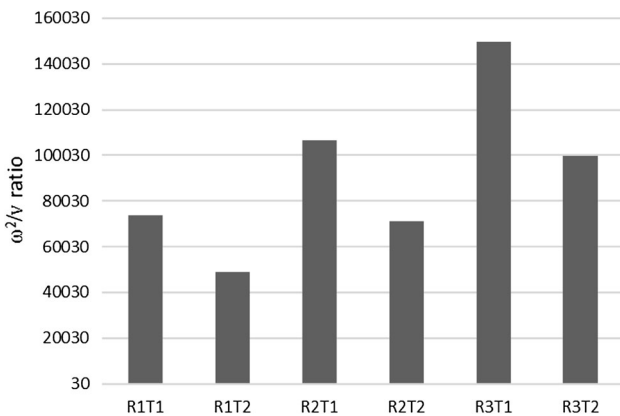


Fig. 17 Comparison of ω^2/ν ratios of the experiments

Table 5 Grain sizes in different zones of the sample R2T1

Sample ID	$\frac{\omega^2}{\nu}$	Nugget zone grain size (μm)	TMAZ grain size (μm)	HAZ grain size (μm)
R1T1	73633.3	2.02	24	30.31
R1T2	49088.89	1.955	22.77	27.24
R2T1	106408.3	2.681	23.22	33.22
R2T2	70938.89	2.497	18.672	30.632
R3T1	149633.3	3.834	21.679	36.42
R3T2	99755.56	2.94	16.556	32.037

TMAZ and base metal of Al side had the maximum hardness amounts (148 and 155 HV, respectively).
 6. The fractography results showed the occurrence of cleavage fracture in all the samples. This subject confirmed the formation of intermetallic compounds in the border zone.

Acknowledgements The authors wish to thank Institute of Iranian National Standards Organization-Mechanical and Metallurgy Research Center and Mr. Derayati for the preparation of project facilities.

References

- Vigh L G, and Okura I, *Mater Des* **44** (2013) 119.
- Fratini L, Buffa G, and Shivpuri R, *Mater Des* **30** (2009) 2435.
- Zhao Y, Zhou L, Wang Q, Yan K, and Zou J, *Mater Des* **57** (2014) 146.
- Hou X, Yang X, Cui L, and Zhou G, *Mater Des* **53** (2014) 106.
- Richter-Trummer V, Suzano E, Beltrão M, Roos A, dos Santos J, and de Castro P, *Mater Sci Eng A* **538** (2012) 81.
- Woo W, Choo H, Brown D W, Feng Z, and Liaw P K, *Mater Sci Eng A* **437** (2006) 64.
- Schenk T, Richardson I, Kraska M, and Ohnimus S, *Comput Mater Sci* **45** (2009) 999.
- Silva A C, Braga D F, de Figueiredo M, and Moreira P, *Mater Des* **55** (2014) 120.
- Mishra R S, and Mahoney M W, *Friction Stir Welding and Processing*, ASM International, New York (2007).
- Zhi-hong F, Di-qiu H, and Hong W, *J Wuhan Univ Technol Mater Sci* **19** (2004) 61.
- Di S, Yang X, Luan G, and Jian B, *Mater Sci Eng A* **435** (2006) 389.
- Gopi S, and Manonmani K, *Sci Technol Weld Join* **17** (2012) 601.
- Forcellese A, and Simoncini M, *Mater Des* **36** (2012) 123.
- Srivatsan T S, Vasudevan S, and Park L, *Mater Sci Eng A* **466** (2007) 235.
- Çam G, and Mistikoglu S, *J Mater Eng Perform* **23** (2014) 1936.
- Fersini D, and Pirondi A, *Eng Fract Mech* **75** (2008) 790.
- İpekoğlu G, and Çam G, *Metall Mater Trans A* **45** (2014) 3074.
- Cui L, Yang X, Xie Y, Hou X, and Song Y, *Mater Des* **51** (2013) 161.
- Liu P, Shi Q, Wang W, Wang X, and Zhang Z, *Mater Lett* **62** (2008) 4106.
- Xue P, Xiao B, Ni D, and Ma Z, *Mater Sci Eng A* **527** (2010) 5723.
- Abdollah-Zadeh A, Saeid T, and Sazgari B, *J Alloys Compd* **460** (2008) 535.
- Tan C, Jiang Z, Li L, Chen Y, and Chen X, *Mater Des* **51** (2013) 466.
- A. Standard. www.astm.org (2011).
- A. Standard. www.astm.org, (2009).
- A. Standard. www.astm.org, (2011).
- Sonne M R, Tutum C C, Hattel J H, Simar A, and De Meester B, *J Mater Process Technol* **213** (2013) 477.
- Xue P, Ni D, Wang D, Xiao B, and Ma Z, *Mater Sci Eng A* **528** (2011) 4683.
- Abbasi M, Taheri A K, and Salehi M, *J Alloys Compd* **319** (2001) 233.
- ASM, ASM metal handbook, Vol 2, 2002 ed., 2002.
- Barekatin H, Kazeminezhad M, and Kokabi A H, *J Mater Sci Technol* **30** (2014) 826.

31. Esmaili A, Givi M B, and Rajani H Z, *Mater Sci Eng A* **528** (2011) 7093.
32. Dilip J, Koilraj M, Sundareswaran V, Ram G J, and Rao S K, *Trans Indian Inst Met* **63** (2010) 757.
33. Pischevar M, Mohandesi J A, Omidvar H, and Safarkhanian M, *J Mater Eng Perform* **24** (2015) 3835.
34. Yu C, Hua D, Li J-z, Zhao J-w, Fu M-j, and Li X-h, *Trans Nonferr Met Soc China* **25** (2015) 2524.